Uncompensated Garnets:
A Magnetic Semiconductor

P.E. Wigen
Department of Physics

DTIC
S ELECTE **D**
NOV 0 2 1995
F

19951101 099

DTIC QUALITY INSPECTED 8

REPORT DOCUMENTATION PAGE

Form Approved
OMB No. 0704-0188

1. AGENCY USE ONLY (Leave blank)	2. REPORT DATE May 9, 1995	3. REPORT TYPE AND DATES COVERED 03/01/91 – 12/31/94	

4. TITLE AND SUBTITLE

Uncompensated Garnets: A Magnetic Semiconductor

5. FUNDING NUMBERS

DAAL03-91-G-0068

6. AUTHOR(S)

Philip E. Wigen, Professor of Physics

7. PERFORMING ORGANIZATION NAME(S) AND ADDRESS(ES)

Department of Physics
The Ohio State University
174 W. 18th Avenue
Columbus, Ohio 43210-1063

8. PERFORMING ORGANIZATION REPORT NUMBER

9. SPONSORING / MONITORING AGENCY NAME(S) AND ADDRESS(ES)

U.S. Army Research Office
P.O. Box 12211
Research Triangle Park, NC 27709-2211

10. SPONSORING / MONITORING AGENCY REPORT NUMBER

11. SUPPLEMENTARY NOTES
The views, opinions and/or findings contained in this report are those of the author(s) and should not be construed as an official Department of the Army position, policy, or decision, unless so designated by other documentation.

12a. DISTRIBUTION / AVAILABILITY STATEMENT

Approved for public release; distribution unlimited.

12b. DISTRIBUTION CODE

13. ABSTRACT (Maximum 200 words)

Yttrium iron garnet (YIG) is a ferrimagnetic oxide, $Y_3Fe_5O_{12}$, and a good insulator. When five to ten percent of the Y^{3+} is replaced by Ca^{2+}, an uncompensated state exists. The resulting material has perturbed magnetic properties, semiconducting electrical properties with activation energies from 0.2 to 0.4 eV and resistivities as low as 300 Ωcm at room temperature, and modified optical properties. In the past year the conductivity studies have concentrated on the evolution of a high conduction state in samples that have been annealed in a reducing atmosphere. The reduction process introduces oxygen vacancies which should compensate the hole introduced by Ca^{2+}. The annealing is also observed to modify significantly the effective exchange constant of the material and the optical activity. These measurements are summarized in this report.

14. SUBJECT TERMS

15. NUMBER OF PAGES

16. PRICE CODE

17. SECURITY CLASSIFICATION OF REPORT UNCLASSIFIED	18. SECURITY CLASSIFICATION OF THIS PAGE UNCLASSIFIED	19. SECURITY CLASSIFICATION OF ABSTRACT UNCLASSIFIED	20. LIMITATION OF ABSTRACT UL

Forward

Yttrium iron garnet (YIG) is a ferrimagnetic oxide, $Y_3Fe_5O_{12}$, and a good insulator. When five to ten percent of the Y^{3+} is replaced by Ca^{2+}, an uncompensated state exists. The resulting material has perturbed magnetic properties, semiconducting electrical properties with activation energies from 0.2 to 0.4 eV and resistivities as low as 300 Ωcm at room temperature, and modified optical properties. In the past three years, the conductivity studies have concentrated on the evolution of a high conduction state in samples that have been annealed in a reducing atmosphere. The reduction process introduces oxygen vacancies which should compensate the hole introduced by Ca^{2+}. The annealing is also observed to modify significantly the effective exchange constant of the material and the optical activity. These measurements are summarized in this report.

Accesion For		
NTIS CRA&I	☑	
DTIC TAB	☐	
Unannounced	☐	
Justification		
By		
Distribution /		
Availability Codes		
Dist	Avail and / or Special	
A-1		

Table of Contents

List of Figures

Figure 16. Optical absorption spectra of Ca0.18:YIG for a sample annealed successively at the indicated temperatures in a N_2 atmosphere.

Introduction

Magnetic YIG single crystal films doped with Ca are being examined as an alternative to the II-VI magnetic semiconductors. Ca:YIG has superior magnetic properties to the II-VI magnetic semiconductors, but it has traditionally been too electrically resistive (10^5-10^6 Ωcm) to be used in practical applications. Under this grant, resistivities as low as 300 Ωcm have been achieved for both as-grown and electrically "pickled" samples. An enhancement of our understanding of the mechanism responsible for the dramatic decrease in the resistivities upon application of a DC electric field (electrical "pickling"), reported eighteen months ago, has been achieved. The data continues to suggest that repulsive trap states are responsible for this effect. Further evidence of these traps have been found in recent optical measurements, which have shown a significant change in the optical absorption upon annealing, including a shift of the band edge by as much as 0.3 eV. It is expected that "pickling" of a reduced film will further alter the optical absorption introducing potentially new optical applications for the material.

A. *Sample Preparation and Characterization*

During the past three years significant effort was directed toward growing good quality YIG films in this laboratory. The temperature profile as well as the long and short term stability of the growth furnace were improved and the impurity content of films grown at different temperatures as well as the saturation temperature for the melt were determined. In addition a Pt stirrer and sample holder for both 3/4" and 1" dia. GGG substrates were fashioned. The films are grown by liquid phase epitaxy (LPE) on (111) oriented single crystal $Gd_3Ga_5O_{12}$ (GGG) substrates. During the past three years 7 Si:YIG discs, 21 Ca:YIG discs, 5 nominally pure YIG disks, and 4 Mg:YIG disks have been grown at this facility.

The crystalline, magnetic, electrical, and optical properties as well as the thickness of each film grown are routinely and thoroughly characterized before proceeding with further examination. The chemical composition of the films is determined by electron probe microanalysis (EPMA) using both computer standards and elemental standards for comparison. The lattice constant of the films is measured by a scanning X-ray diffractometer with a computer-controlled sample chamber to easily orient the single crystal films. The magnetization of the films is measured from 4 K to the Curie temperature by a Foner type vibrating magnetometer, and the electrical resistivity and activation energy are measured from 150 K to 300 K.

The optical absorption of the films is measured from 400 nm to 2500 nm, and the interference fringes in that region are used to determine the film's thickness to an accuracy around 3%. The film thickness has also been measured by a scanning electron microscope which shows a film-substrate contrast when examining the film-substrate cross section. The contrast is due to the lower conductivity of the GGG substrate; this second technique has an accuracy nearer 5% and is reserved as a check for the optical method.

B. *Trap-Filled-Limited Surface Layer*

The Log(I) vs. Log(V) curve of Ca:YIG is not quite ohmic even at small applied electric fields (<100 V/cm). A typical Log(I) vs. Log(V) curve for the $Ca_{0.2}$:YIG films grown in this laboratory is shown in Figure 1 [1]. For very small fields («100 V/cm) the slope is 1.02, at fields around 100 V/cm the slope increases to 2, and at fields near 10^4 V/cm the slope approaches 1.2.
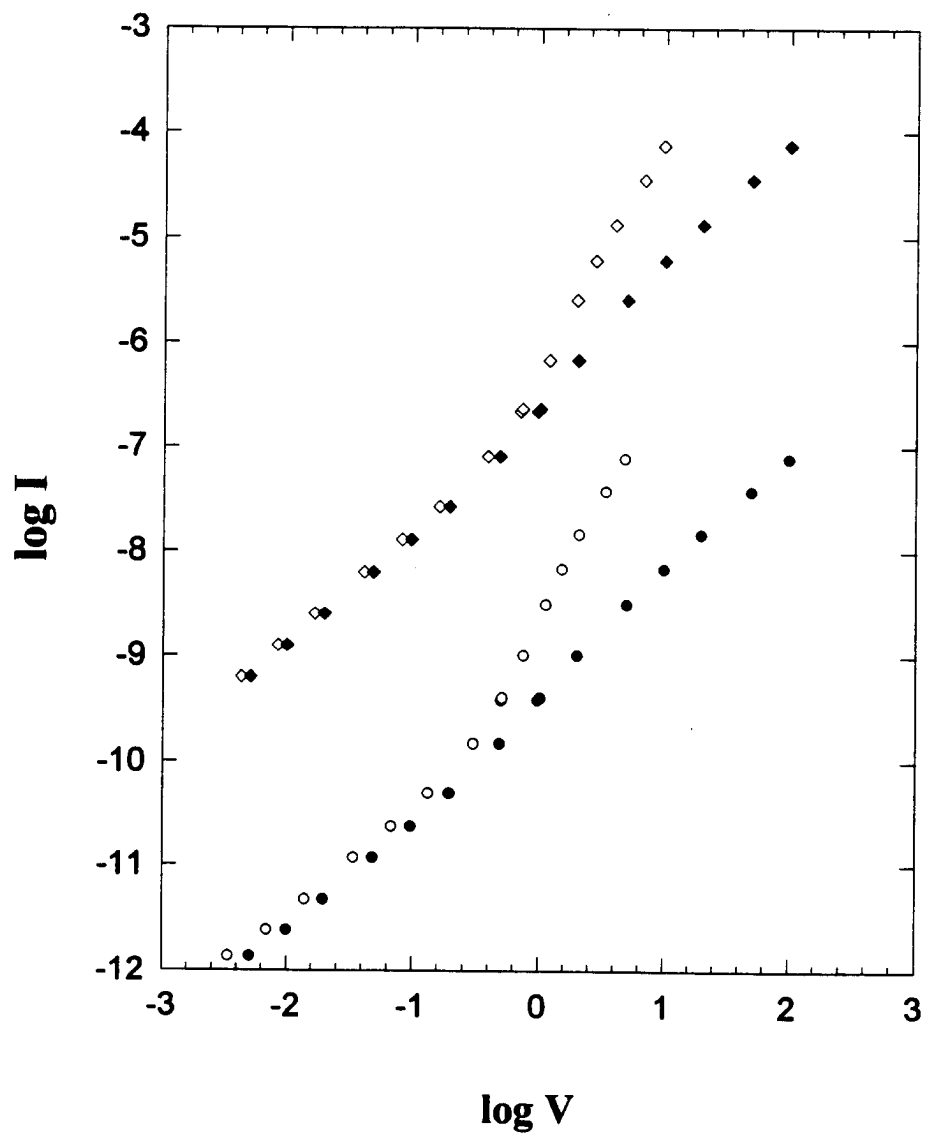
Fig. 1. Typical I-V characteristic showing non-ohmic behavior in the raw data (filled symbols) and trap-filled-limit behavior (slope =2) in the fitted surface layer signal (open symbols) at two different temperatures: ◇ 240 K, and ○ 160 K.

A two layer model was proposed by Larson and Metselaar in 1973 to account for this effect [2], but the nature of the thin surface layer in this model has remained unclear.

The research on the electrical properties of Ca:YIG conducted by this group over the past three years has led to the conclusion that the conduction state of the surface layer is the Trap-Filled-Limited (TFL) state even at very low applied voltages. The TFL state is characterized by the slope of the Log(I) vs. Log(V) curve equaling 2.0 regardless of the energy distributions of the particular electron traps. The raw data in figure 1 were fit to the equation:

$$V = V_B + V_S = RI + \alpha I^{0.5} ,$$

where R is the resistance of the bulk and α is a constant which depends on the total number of traps in the surface layer. The voltage drop across the surface layer, V_S, could then be separated from the raw data and is included in figure 1. The slope of the log I vs. Log V curve for the surface layer thus determined varied between 1.9 and 2.1, in good agreement with the value of 2.0 expected for TFL charge transfer. This fit performed on a number of typical Ca:YIG samples also showed the conductivity of bulk YIG to be 1000 times greater than that of the surface [1].

This analysis also shows that for fields near or below 100 V/cm the voltage drop across the surface layer can be 80 to 90 percent of the total drop, effectively masking the bulk signal. For fields of 10^4 V/cm the voltage across the surface layer is only 10 to 20 percent of the total applied voltage, and the bulk signal dominates. These ratios are also temperature dependent; at lower temperatures the bulk signal comprises more of the total at all applied voltages.

The ability to separate the bulk signal from the raw data represents an important step forward in the understanding of all electrical measurements on Ca:YIG. It is believed by this group that this is the first time the TFL conducting state for the surface layer has been proposed to explain the anomalous electrical behavior of M^{2+}:YIG films, where M^{2+} refers to a divalent metallic ion.

C.   Oxygen Vacancy Study

1.   Annealing conditions

In an effort to better understand the electron trap levels in the high conduction state, the charge compensation mechanism in the normal conduction state, and the low temperature magnetization anomaly in M^{2+}:YIG, a systematic study was carried out to determine what role, if any, oxygen vacancies play in these phenomena [1]. $Ca_{0.2}$:YIG films were annealed for 7 hours in a flowing nitrogen atmosphere at 600 C, 800 C, 900 C, 960 C, and 1000 C to determine the onset temperature of additional oxygen vacancy creation and their subsequent effects on the magnetic and electrical properties of the films. $Ca_{0.2}$:YIG films were also annealed for 7 hours in a flowing oxygen atmosphere at 1000 C, 1100 C, and 1200 C in order to insure that any observed changes in the films' properties were indeed due to oxygen vacancy creation and not purely thermally activated. The magnetization, I-V curve, lattice constant, and optical absorption were then remeasured to detect any changes induced by the creation of oxygen vacancies [1].

2.   Changes in magnetic properties

As can be seen in Figure 2, the changes in the magnetization were dramatic. For the sample annealed in nitrogen at 1000 C, the $4\pi M_s$ at 4 K decreased almost 600 Gauss from its as-grown value of 2600 Gauss, the film's magnetization decreased by 20 to 50 percent over the
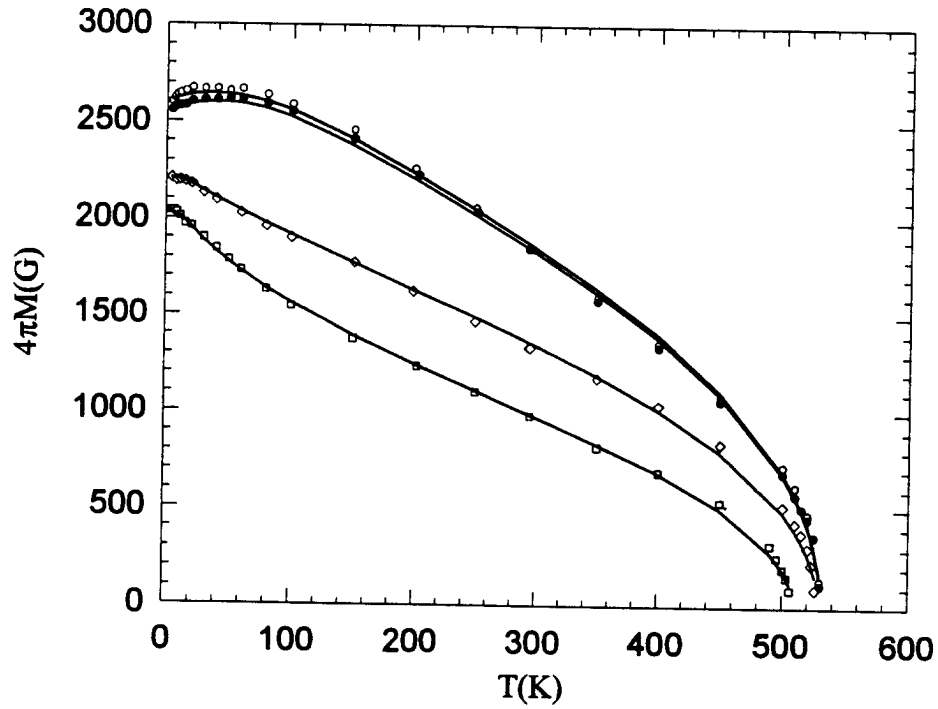
Figure 2. Data and theoretical fit for the temperature dependence of the magnetization for $Ca_{0.20}$:YIG. The calculated values are illustrated with solid lines. The symbols for the experimental results are as follows:

| ○ | 1000 C in O_2, | • | 900 C in N_2, |
| ◇ | 960 C in N_2, | and ▫ | 1000 C in N_2. |

entire temperature range from 4 K to the Curie temperature, the Curie temperature decreased by 30 K, and a change in the general shape of the magnetization curve is observed. Moreover, the magnetization curves of the sample annealed at 900 C and 960 C show a smooth transition from the as-grown curve to that of the sample annealed at 1000 C.

3. Changes in electrical properties

As shown in Figure 3, an equally dramatic change in the films' electrical properties occurred as the annealing temperature was successively increased. The room temperature resistivity of the sample annealed at 1000 C was 10^7 times larger than its as-grown value, and the activation energy of its conductivity was three times larger than that of the as-grown state.

4. Lattice constant changes

The lattice constant of the films annealed in nitrogen were observed to decrease continuously and markedly from 12.390 Å to 12.358 Å as the annealing temperature increased, suggesting that oxygen atoms were indeed removed from the lattice. On the assumption that the inverted spins responsible for the decrease in the magnetization at 4 K are induced by the creation of singly charged oxygen vacancies $[V_o^*]$ in the nitrogen annealing, the number of such singly charged oxygen vacancies was calculated for each of the films. This calculation of the $[V_o^*]$ concentration for the $Ca_{0.20}$:YIG films showed an increase from 0.03 formula units in the as-grown state to 0.16 formula units for the film annealed at 1000 C in N_2

5. Oxygen Annealing

On the other hand, the films annealed at 1000 C and 1100 C in an oxygen atmosphere showed no change in the lattice constant, and the film annealed at 1200 C in oxygen showed a slight decrease from 12.384 A to 12.381 A, possibly due to a change in impurity Pb ion valency. Thus even at temperatures up to 1200 C the oxygen annealing produced virtually no oxygen vacancies and only slight changes in the magnetization, which strongly suggests that the drastic effects observed in the nitrogen annealed samples were not purely thermally activated reorientation but were indeed due to the creation of oxygen vacancies in the lattice.

6. Interpretation of Magnetic Results

To explain the surprising changes in the magnetization of the annealed films, a model proposed by A. Lehmann-Szweykowski [3] was adopted wherein a singly charged oxygen vacancy can mediate a ferromagnetic superexchange interaction between its neighboring Fe^{3+} ions. The oxygen atoms in YIG and substituted YIG films are known to mediate an antiferromagnetic Fe-O-Fe superexchange interaction. When these oxygen atoms are removed by annealing in nitrogen atmosphere, they leave behind an oxygen vacancy in the lattice and one unpaired electron from each of the neighboring Fe^{3+} ions. These electrons are available to be trapped at this or other oxygen vacancies.

If each electron trapped at an oxygen vacancy mediates a ferromagnetic superexchange interaction between its two neighboring Fe^{3+} ions, the process as a whole has the effect of flipping the magnetic moment of the tetrahedral Fe^{3+} ion [1]. The low temperature magnetization anomaly in Ca:YIG can then be explained solely by the presence of singly charged oxygen vacancies, V_o^*. A quantitative model, based on a microscopic Heisenberg Hamiltonian, was constructed to take into account the different local environments of oxygen sites due to lattice imperfections in the crystal, and to calculate the effects on the magnetization of oxygen vacancies at these different sites with zero, one, and two trapped electrons. Using this molecular field model the magnetization vs. temperature graphs for the samples annealed in nitrogen were fit

5
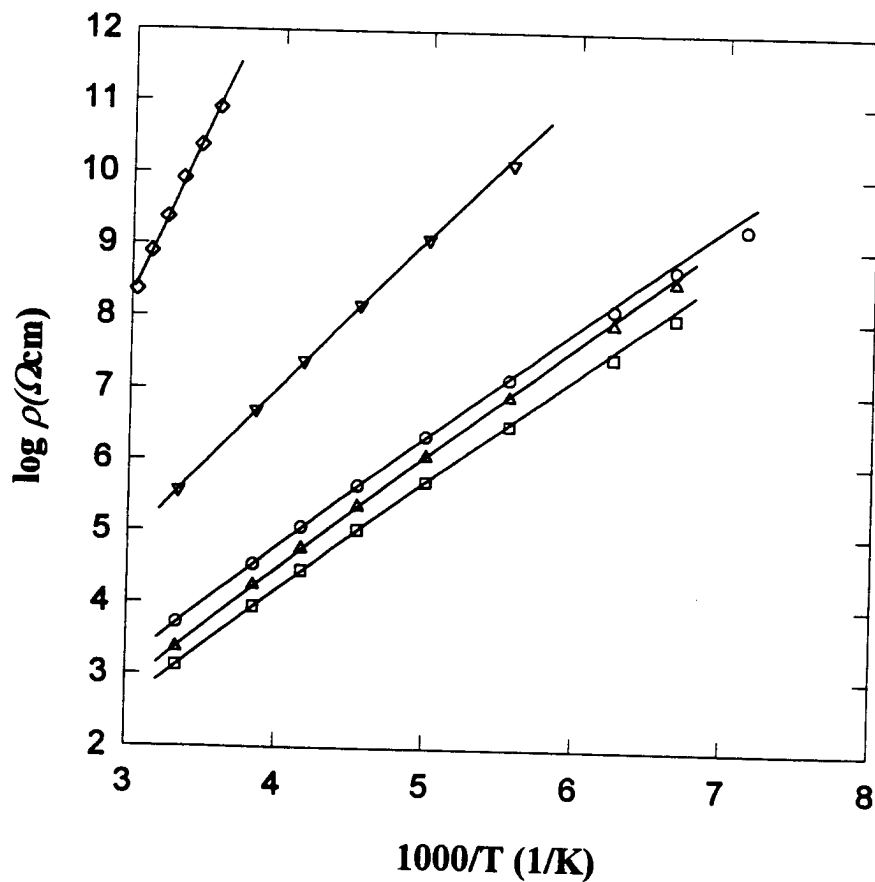
Figure 3. Data and theoretical fit for the temperature dependence of the resistivity for $Ca_{0.20}$:YIG. The calculated values are illustrated with solid lines; The symbols for the experimental results are as follows:

○ as grown, □ 1000 C in O_2, ▽ 960 C in N_2,
△ 900 C in N_2, and ◇ 1000 C in N_2.

theoretically to very good agreement as shown by the solid lines in Figure 3.

The low temperature magnetization anomaly, in which the saturation magnetization decreases with decreasing temperature below about 60 K, has been thought to be exclusively due to the presence of Fe^{4+} or O^- charged centers. This would place the sample exhibiting this anomaly within the undercompensated region of the electronic phase diagram (Figure 4). This annealing study showed that the anomaly can exist in the overcompensated region as well. This provides an alternative explanation for the low temperature anomaly. It was, in fact, determined by this study that the $Ca_{0.2}$:YIG films were in the overcompensated region even in the as-grown state.

7. Interpretation of electrical results

To explain the drastic changes in the electrical conductivity and activation energy of the Ca:YIG films annealed in nitrogen, the existence of an impurity band was proposed which is located 0.3 eV above the valence band with a half-width of 0.1 eV [1]. The fit to the data resulting from this hypothesis is shown in Figure 3. It is believed that this impurity band corresponds to the occupation of oxygen vacancies by one electron. Each oxygen vacancy created during the annealing process leaves behind two unpaired electrons, and while one of them may often fill the lattice site of the missing oxygen atom, both electrons occupying that site is energetically unfavorable.

The annealing in nitrogen thus creates a process whereby excess electrons generated are both filling trap states and recombining with valence holes, which explains the increase in both the electrical resistivity and activation energy. The fact that two electrons are created by each oxygen vacancy and as much as 0.13 formula units (5×10^{20} cm^{-3}) of singly charged oxygen vacancies were created during annealing explains the magnitude of the change in these parameters. Similar conductivity changes have been observed in insulating MgO single crystals when annealed at 800 C in vacuum; in that material the charge conduction mechanism was identified as mobile oxygen holes in excess of 10^{20} cm^{-3} [4].

Finally, this group has observed that the optical absorption spectra of these Ca:YIG films exhibit two broad peaks, one near 600nm (2.07eV) and the other smaller one near 900nm (1.4eV), with a band gap energy around 2.5 eV. This suggests the existence of trap bands centered at 0.4 eV and 1.1 eV above valence band. These may well correspond to oxygen vacancy bands with one and two trapped electrons respectively. The absorption spectra of the samples annealed in nitrogen show increased absorption and spreading of these peaks, consistent with the idea of the singly charged oxygen vacancy bands increasing in occupancy.

8. Room Temperature High Conduction State (RTHCS)

If the deep repulsive trap in the high conduction state of Ca:YIG corresponds to the occupation of singly charged oxygen vacancies, V_o^*, by a second valence electron, then the creation of many such V_o^* centers during the annealing in nitrogen should increase the capture cross section for the repulsive trap, thus making it easier to enter the high conduction state.

Figure 5 displays the recent discovery that the continuous application of 100 V DC (10^4 V/cm) at room temperature and in vacuum to the $Ca_{0.2}$:YIG samples annealed at 960 C and 1000 C in nitrogen induces a room temperature high conduction state (RTHCS). It is believed that this RTHCS uses the same mechanism, repulsive electron traps, as the previously discovered low temperature high conduction state (LTHCS) [5], but with deeper trap levels which are stable at room temperature.

7

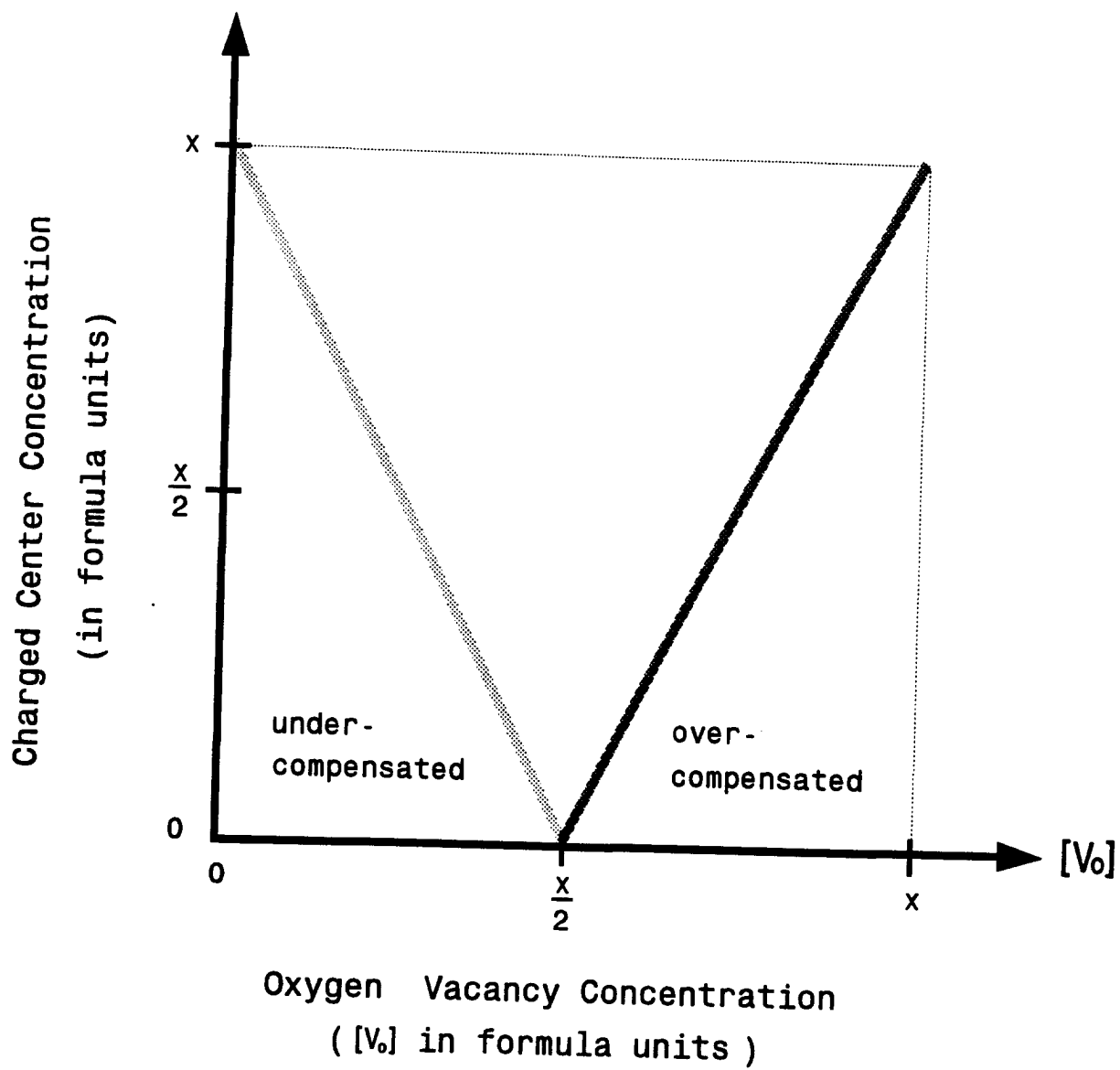Fig. 4. Electronic Phase Diagram for $M_x : Y_{3-x} Fe_5 O_{12-[V_o]}$

$\cdots$ $[Fe^{4+}] + [O^-]$ $\quad$ $\blacksquare$ $[V_o^{\cdot}]$

8
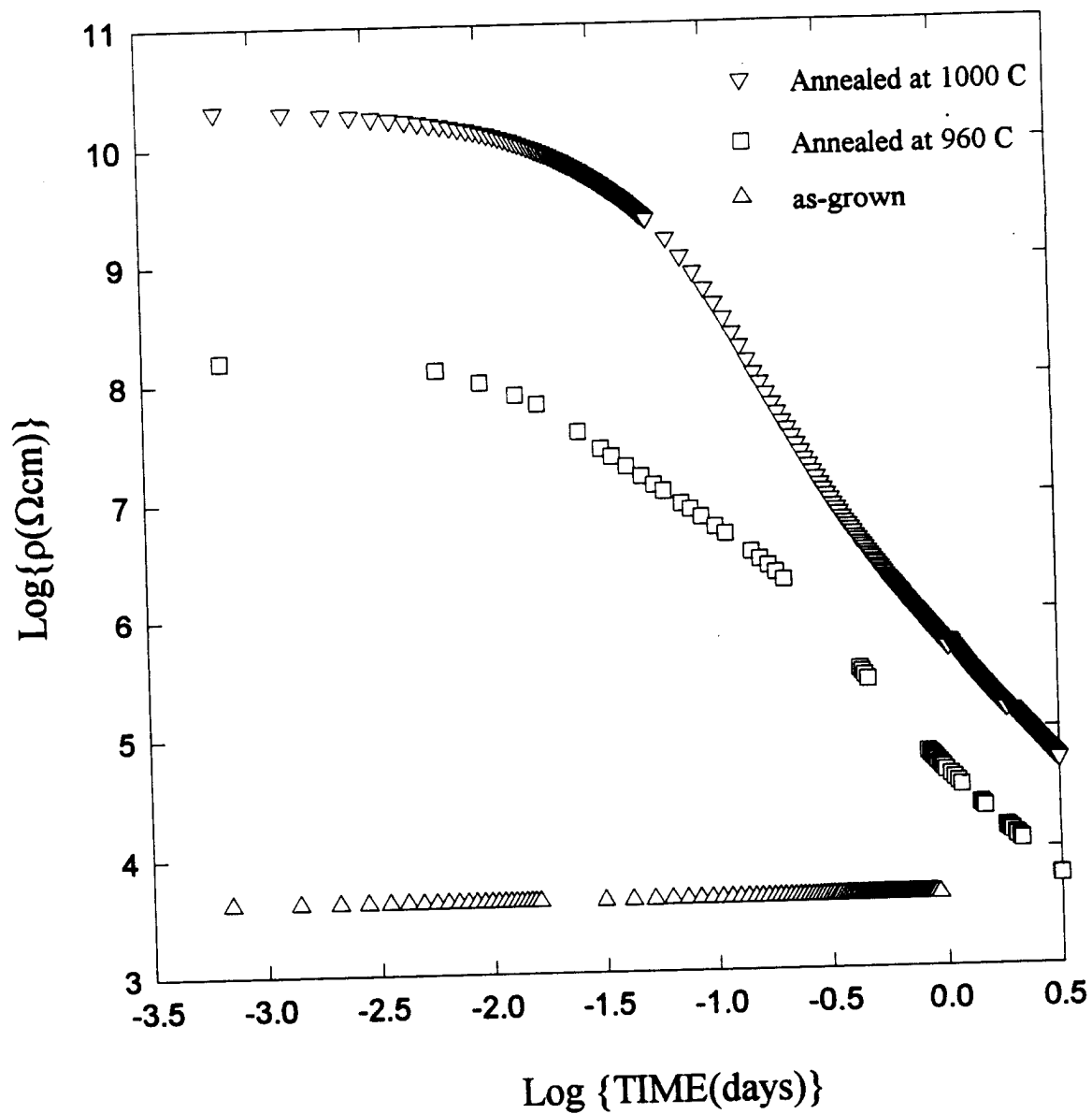
Fig. 5. The dependence of the resistivity decay process on different annealing conditions [E = 10^4 V/cm (100 V), T = 300 K]

The room temperature experiment carried out on an identical unannealed sample (with 0.03 formula units of singly charged oxygen vacancies) for more than twenty hours produced no change in the conductivity. For these same conditions the conductivity of the film containing 0.12 f.u. of singly charged oxygen vacancies increased by five orders of magnitude during six days of application. Finally, the conductivity of the film containing 0.15 f.u. of singly charged oxygen vacancies increased five orders of magnitude in just one day with an additional order of magnitude increase over the next five days.

The film with 0.12 f. u. of singly charged oxygen vacancies arrived at a resistivity of 1.70×10^3 Ωcm after six days, roughly half of its as-grown value. The applied voltage was then removed, and its resistivity was monitored for several minutes each day for three days and found to relax during the first day to 2.2×10^3 Ωcm, still less than its 3.1×10^3 Ωcm as-grown value, and remained constant thereafter. The applied voltage was then applied again for an additional four days (not included in Figure 5), during which time the film's resistivity decreased steadily to 750 Ωcm. In subsequent experiments the resistivity was reduced further to 300 Ωcm.

There is a clear indication in this experiment that oxygen vacancy concentration is a critical parameter. It is postulated that the huge increase in conductivity in the annealed samples is due to the large number of singly occupied oxygen vacancies available, and that in the presence of the applied electric field ($\sim 10^4$ V/cm) valence electrons tunnel into trap states at the singly charged oxygen vacancy sites, leaving behind holes in the valence band which contribute to conduction.

The room temperature resistivity of the films used in the initial LTHCS study were all greater than 10^5 Ωcm, with the $Ca_{0.08}$:YIG being the most resistive at 10^9 Ωcm. Further, the LTHCS was induced at low temperature where the resistivity was many orders of magnitude larger, so the LTHCS films never achieved resistivities lower than 10^4 Ωcm. The RTHCS induced in the annealed films represents a decrease by more than a factor of ten over the resistivity of the as-grown normal state; the experiment was stopped only due to the inability of the electrometer in use to supply more than 2.5 mA. At the point in the experiment when this limiting current was reached, the conductivity was still increasing. It seems quite possible that further conductivity increases of one or even two orders of magnitude could be achieved.

9.   *Temperature and Voltage study of RTHCS*

With the assumption of deep trap levels as the basis for the RTHCS, a voltage and temperature dependence for the effect would be expected. To test this expectation, a film annealed at 960°C was examined at room temperature for different electric fields (Fig. 6), and another film annealed at 1000°C was examined at an applied electric field of $\sim 2 \times 10^4$ V/cm (200V) for different temperatures (Fig. 7). In both cases the resistivity of the films analyzed had been decreased to near or below the as-grown value, so the region in Fig. 5 analyzed was linear and the percent change in the resistivity over the course of each "pickling" run was small ($\sim 10\%$). The decrease in the resistivity over the whole experiment was small enough ($\sim 50\%$) in both these figures that its effect on the rate dependence was assumed to be negligible. At the end of the applied field dependence study the resistivity of the sample annealed at 960°C had reached a value of 300 Ωcm, a factor of ten smaller than its as-grown value. In these figures the resistivity at the start of each respective run is normalized to one, and the slope of each curve measures the relative rate of the resistivity decay as a function of either applied voltage or temperature. The

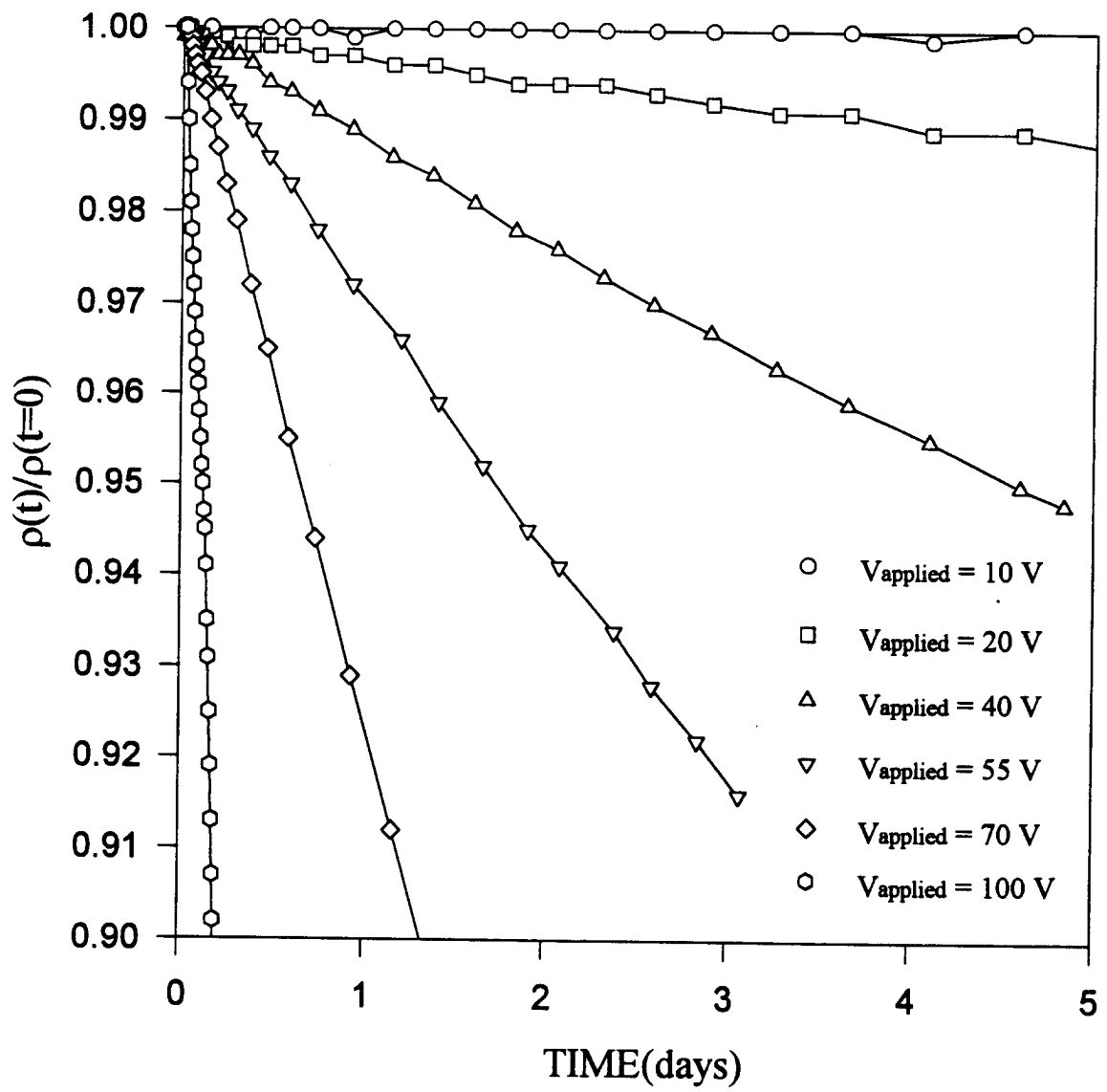Fig. 6. The dependence of the relative resistivity decay rate on the applied electric field
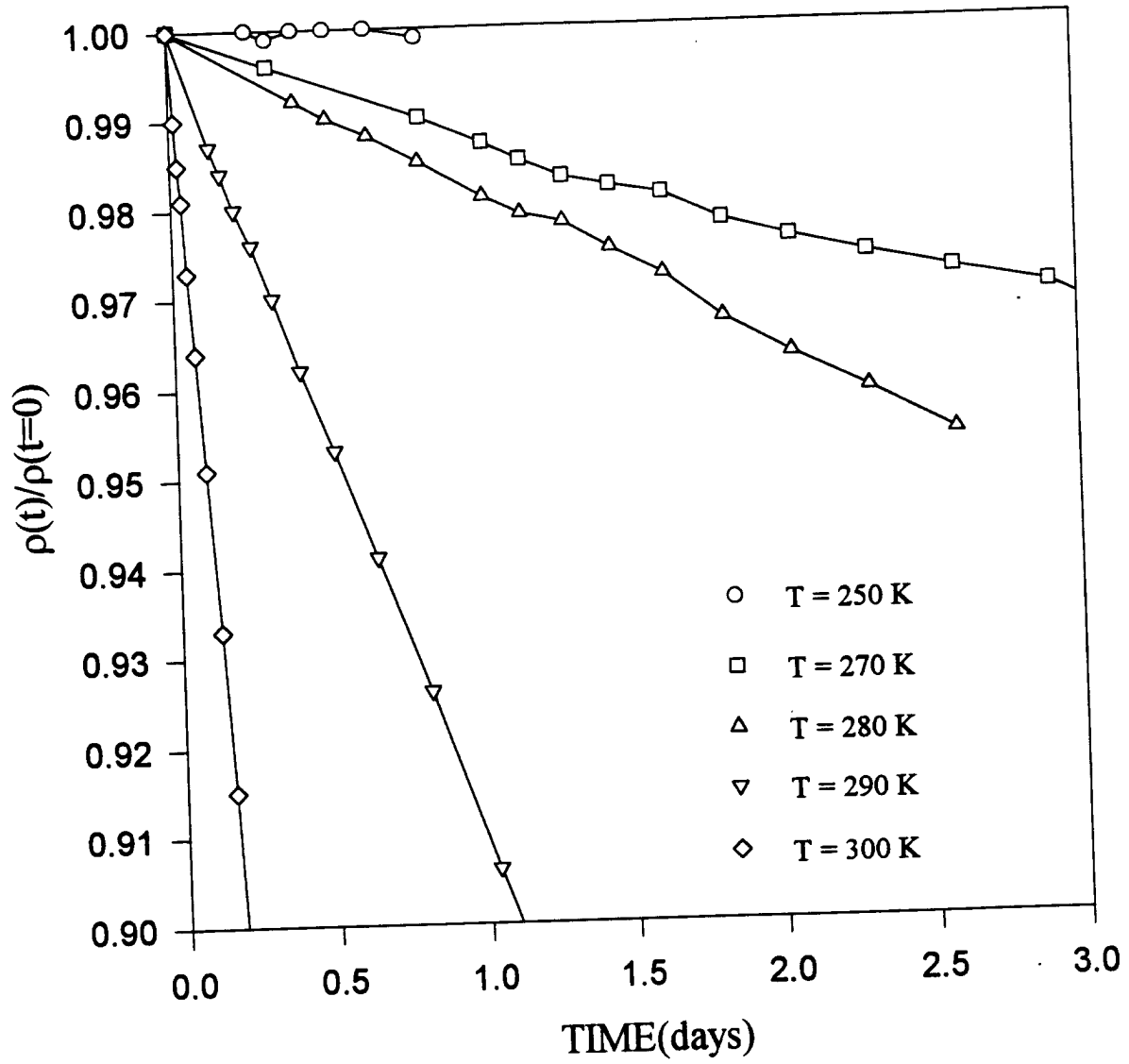
[Annealed at 960 C, T = 300 K]

Fig. 7. The dependence of the relative resistivity decay rate on temperature
[Annealed at 1000 C, E = 2x10^4 V/cm (200 V)]

relative resistivity decay rate thus determined was found to depend exponentially both on $V_{applied}$ and 1/T to very good agreement.

The zero slope of the $V_{applied}$ = 10 V curve in Fig. 6 suggested that there might be a threshold field between 2.4×10^3 V/cm (20 V) and 1.2×10^3 V/cm (10 V), below which no reduction in the resistivity was possible. To test this hypothesis a third film which had been annealed at 1000°C in N_2 was subjected to a field of 1.2×10^3 V/cm (10 V) for sixty days, during which time the resistivity decreased more than four orders of magnitude (Fig. 8). This clearly demonstrates that the fundamental process responsible for the resistivity decrease is not a threshold phenomenon, but is rather a statistical event whose probability diminishes continuously (exponentially) with decreasing voltage (and temperature). In addition, the shapes of the $V_{applied}$ = 100 V and $V_{applied}$ = 10 V curves shown in Fig. 8 have the same form, if the curve for $V_{applied}$ = 10 V is shifted by negative Log{100} along the Log{TIME} axis. This illustrates the existence of a universal decay curve independent of applied electric field, indicating that the same process is occurring in both cases, but that the statistical event responsible is 100 times more likely with $V_{applied}$ = 100 V than with $V_{applied}$ = 10 V.

Both the dramatic decreases in the resistivity and the activation energy as well as the temperature and applied voltage dependence of the resistivity decay rate suggest that the phenomenon responsible is the tunneling of valence electrons into repulsive trap states in the crystal. Removing electrons from the valence band, where the charge conduction is occurring, into deep trap states would result in decreases in both the resistivity and activation energy. If those trap states were also surrounded by a repulsive coulombic barrier, the initial (linear) rate of the resistivity decay would be expected to have the following functional dependence on the temperature and applied electric field,

$$\frac{d\rho}{dt} \propto \exp\left[\frac{U_{carrier} - \Phi}{k_BT}\right] \tag{1}$$

where ρ is the electrical resistivity, $U_{carrier}$ is the statistical average of the kinetic energy of the charge carriers and is proportional to the applied electric field, Φ is the energy of the repulsive trap barrier ($U_{carrier} - \Phi < 0$), k_B is Boltzmann's constant, and T is the temperature. For small variations in ρ, $d\rho/dt$ will be directly proportional to the probability of electron trapping, and (1) is in full agreement both with the experimental data in Fig. 6 and Fig. 7 and elementary Fermi-Dirac statistics for quantum tunneling through a repulsive barrier.

The specific nature of the repulsive trap is difficult to determine. It is most likely an impurity state, which are numerous in both quantity ($\sim 10^{20}$ cm^{-3}) and type in uncompensated garnets. Using equation (1) as an Ansatz, a detailed model of the trapping kinetics has been developed which accurately reproduces the shape of the resistivity decay process measured experimentally, as shown in Fig. 8.

A further indication of carrier trapping in these materials comes from the low temperature measurement of the activation energy (Fig. 9). During the initial reduction in temperature from 300 K to 40 K, the graph of Log{Resistance} vs. 1/T behaved linearly as expected down to 100 K. Near 100 K the measured current became comparable to the leakage current of the electrical circuit ($\sim 10^{-12}$ Amps), and the graph leveled off. Upon increasing the temperature from 40 K,

13
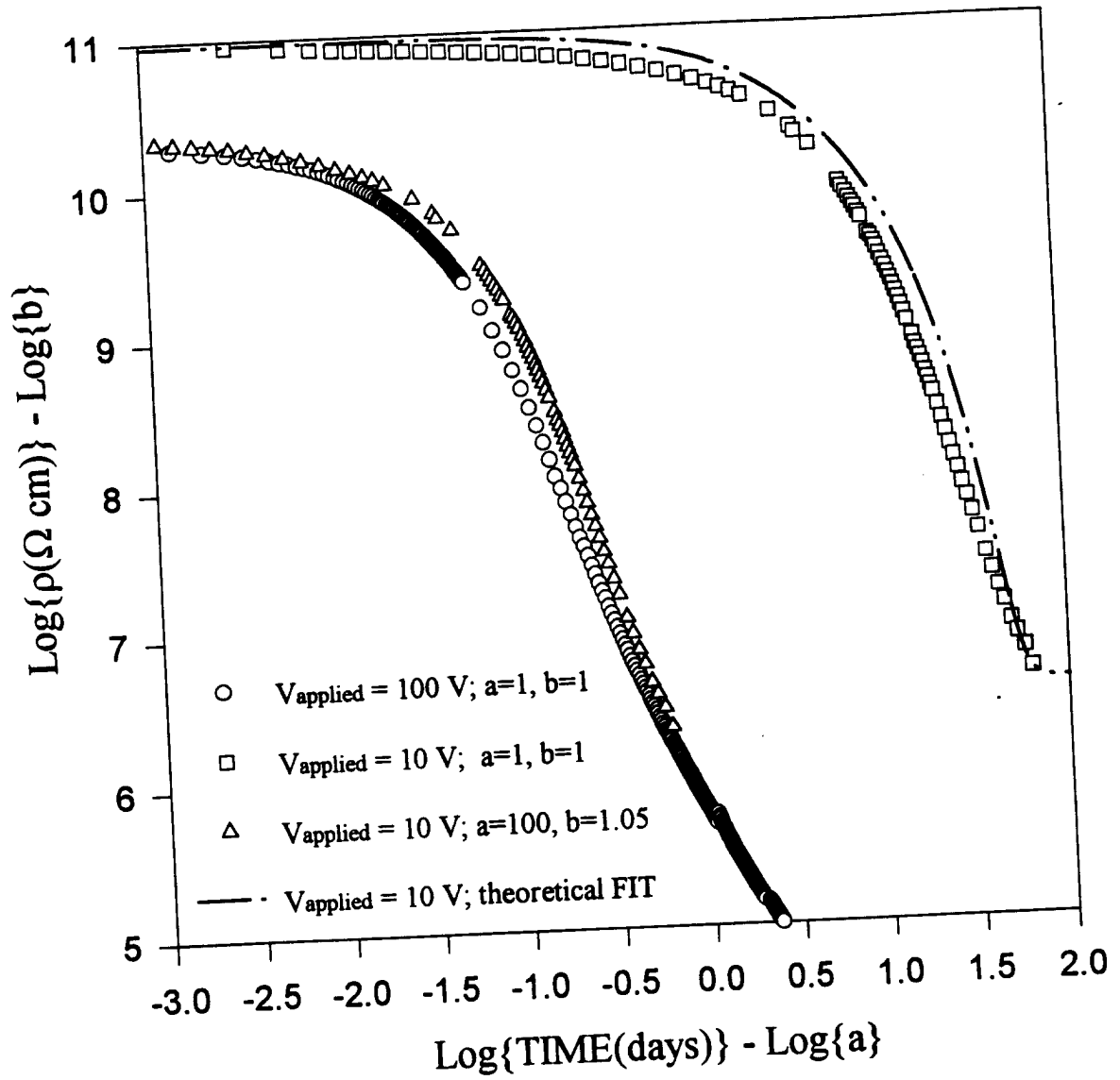
Fig. 8. Similarity of resistivity decay curves for $E = 10^4$ V/cm (100 V) and $E = 10^3$ V/cm (10 V), arising from a universal decay curve illustrated by the Log{a} and Log{b} transformation. Also pictured is the agreement between the 10 V curve and the detailed theoretical fit.
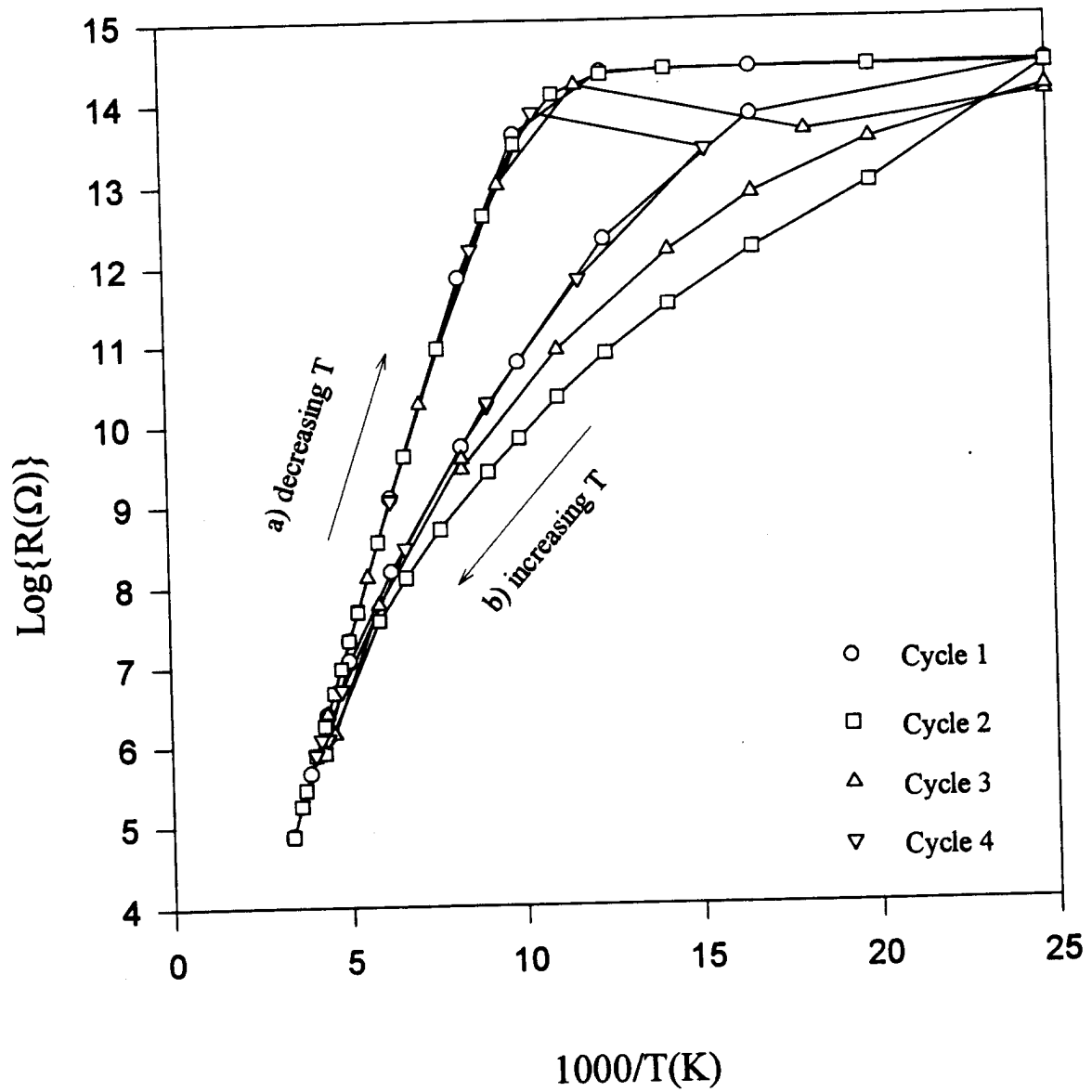
Fig. 9. Log{Resistance} vs. 1000/T showing a consistent electrical activation energy for decreasing temperature but a hysteresis for increasing temperature less than 230 K.

15

both the value of the resistance and the slope of the Log{Resistance} vs. 1/T graph (∝ activation energy) were considerably smaller than the values measured for decreasing temperature. When the temperature was raised above 235 K the film reverted to its initial state and the same (high) resistances and slope are then observed all the way back down to 100 K. This suggests the existence of shallow repulsive trap sites, into which electrons can tunnel at temperatures below 100 K, but which become thermally vacated for T > 230 K. The thermal cycling effect in Fig. 9 has been observed both in as-grown and "pickled" films, so it would seem that the shallow traps responsible are not created by the annealing or the electrical "pickling" processes. This may be related to a similar low temperature high conduction state in as-grown Ca:YIG films which was induced by high electric fields and/or optical pumping as reported by Yuan, for which shallow repulsive traps were the proposed mechanism [5].

D. Related Phenomena

The significant changes in electrical, magnetic, and optical properties of the Ca:YIG films produced by annealing lead to an investigation by this group of the effects annealing had on a significantly different compound to see if the conclusions of the annealing study held under more general conditions. A sample of composition $Bi_{0.09}Tm_{2.14}Pb_{0.06}Ga_{1.9}Fe_{3.1}O_{12}$ was studied in cooperation with Airtron, Inc. which is a subdivision of Litton, Inc.. This material is a bubble type domain material and is used in a commercial crack detector [6]. It was found that annealing the sample in an oxidizing or reducing environment had a profound effect on the magnetic properties and could be used to "set" the desired magnetic properties needed for the operation of the device thus improving the yield of the material. In the sample investigated, an oxidation treatment increased the value of the magnetization at high temperature but decreased it at low temperature. This material was found to undergo a second order phase transition involving the easy direction of magnetization as shown in Figure 10 [7]. Specifically, the easy direction of magnetization was found to reorient itself from easy plane to easy axis as the temperature of the sample was raised from 4.2 K up to room temperature. The temperature range of the transition deceased from roughly 130 to 150 K to 100 to 120 K upon annealing. The material has a compensation point which decreased from 220 K to 196 K upon annealing.

The property changes this material underwent upon annealing are also evident by the significant changes observed in the internal anisotropy fields. Upon moving through a magnetic compensation point, the dominant magnetic sublattice changes. The changes in the magnetization on annealing, indicate that the tetrahedral sublattice magnetization increased.

E. Ferromagnetic Resonance

Ferromagnetic resonance (FMR) measurements may be combined with the magnetization measurements to determination the internal anisotropy fields, the effective g-value, and the spin-wave dispersion coefficient of the material.

The annealing conditions examined were the same as those which produced broad changes in the resistivity and the magnetization, namely at high temperatures (T > 900 C) in a N_2 atmosphere for long time periods of time (> 7 hours). The magnetic and electrical properties measured for these high temperature annealings are significantly different than the previous measurements made by this group [8] using a low temperature annealing treatment (a boiling $FeCl_2$ solution) and by other groups [9] (performing the annealing in Ar at 870 C) indicating that the annealings affect the samples differently.
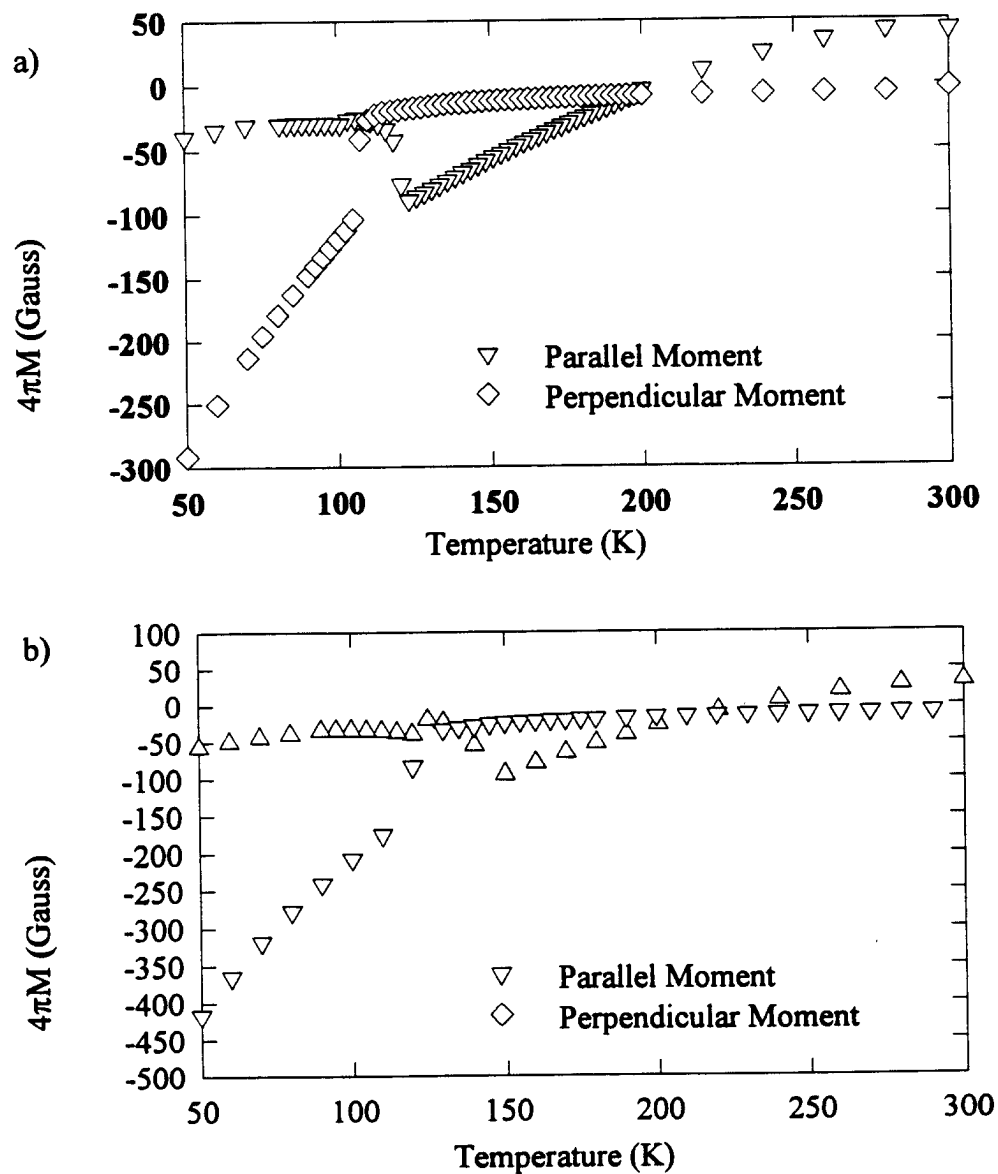
16

Figure 10. Temperature Dependence of the Magnetization
in zero applied field for an a) annealed sample
and b) unannealed Sample of $Bi_{0.8}Tm_{2.14}Pb_{0.06}Ga_{1.9}Fe_{3.1}O_{12}$.

Figure 11a shows the effects of the high temperature annealing on the effective anisotropy field (which is a measure of the magnetization of the film) of a Ca:YIG sample. The results are consistent with measurements of the magnetization under different high temperature annealing conditions made by Song [1]. Both Song's magnetization studies and effective field results, shown in figure 11a, are different from those obtained by Hsai using $FeCl_2$ in a low temperature annealing [8]. Hsai found little if any change in the magnetization and a slight increase in the effective anisotropy field of his films. These differences seem to be due to the low and high temperature annealings resulting in markedly different numbers of oxygen vacancies being formed. Analysis of the samples upon annealing at 1000 C has shown cracking on the surface of the film. Such cracking is consistent with a large number of oxygen vacancies being formed and decreasing the lattice constant sufficiently to produce high stress levels in the crystal lattice. Measurements of the lattice constant of the annealed films support this observation. Upon annealing at 1000 C, the lattice constant was found to decrease by .02 angstroms, which is a sufficient mismatch to cause cracking in as grown films. Such cracking is not observed in the low temperature annealed samples.

Changes in the FMR linewidth, shown in figure 11b, and the effective g-value, shown in figure 12a, also occur for the different annealing conditions. Hsai found that for low temperature annealing, the linewidth became narrower, while as observed in figure 12a, the high temperature annealing produced a larger linewidth. The high temperature annealing may result in a more disordered structure (due to the additional oxygen vacancies), which would tend to broaden the linewidth, compared to films reduced at low temperatures. Similarly, the g-value changed differently for the two annealing conditions. While a lower temperature annealing in an Ar atmosphere at T=870 C resulted in a decrease in the g-value [9], the high temperature annealing resulted in an increase as seen in figure 12a. The added disorder produced by the extra oxygen vacancies would further break the orbital symmetry of the Fe^{3+} and increase the spin-orbit contribution to the angular momentum contribution to the g-value. This results in a larger g-value as observed.

One unexpected result is that for both the low temperature and high temperature annealings, the effective exchange constant increased as shown in figure 12b. The effective exchange constant increased by roughly 20 % for the low temperature annealing done by Hsai, and by 167 % for the high temperature annealing. The large magnitude of increase observed after the annealing is highly unusual and will be investigated further. Should this be found to be dependent on the annealing temperature, it would allow for the dispersion relation governing the exchange modes to be modified in a controlled fashion.

F.   *Optical*

In an attempt to ascertain a comparison with the optical properties, photoinduced absorption experiments were undertaken [10]. The pumping light had a wavelength of 365 nm (3.4 eV). The photoinduced absorption was taken as a function of temperature, energy, frequency of the optical pump modulation, and intensity.

The temperature dependence of the photoinduced absorption was found to have an exponential dependence on temperature and has a characteristic temperature θ_o of 25 K, the same θ_o determined from the anomaly in the magnetization's temperature dependence.

The energy dependence of the photoinduced absorption displays two peaks as can be seen

18

(a)

(b)
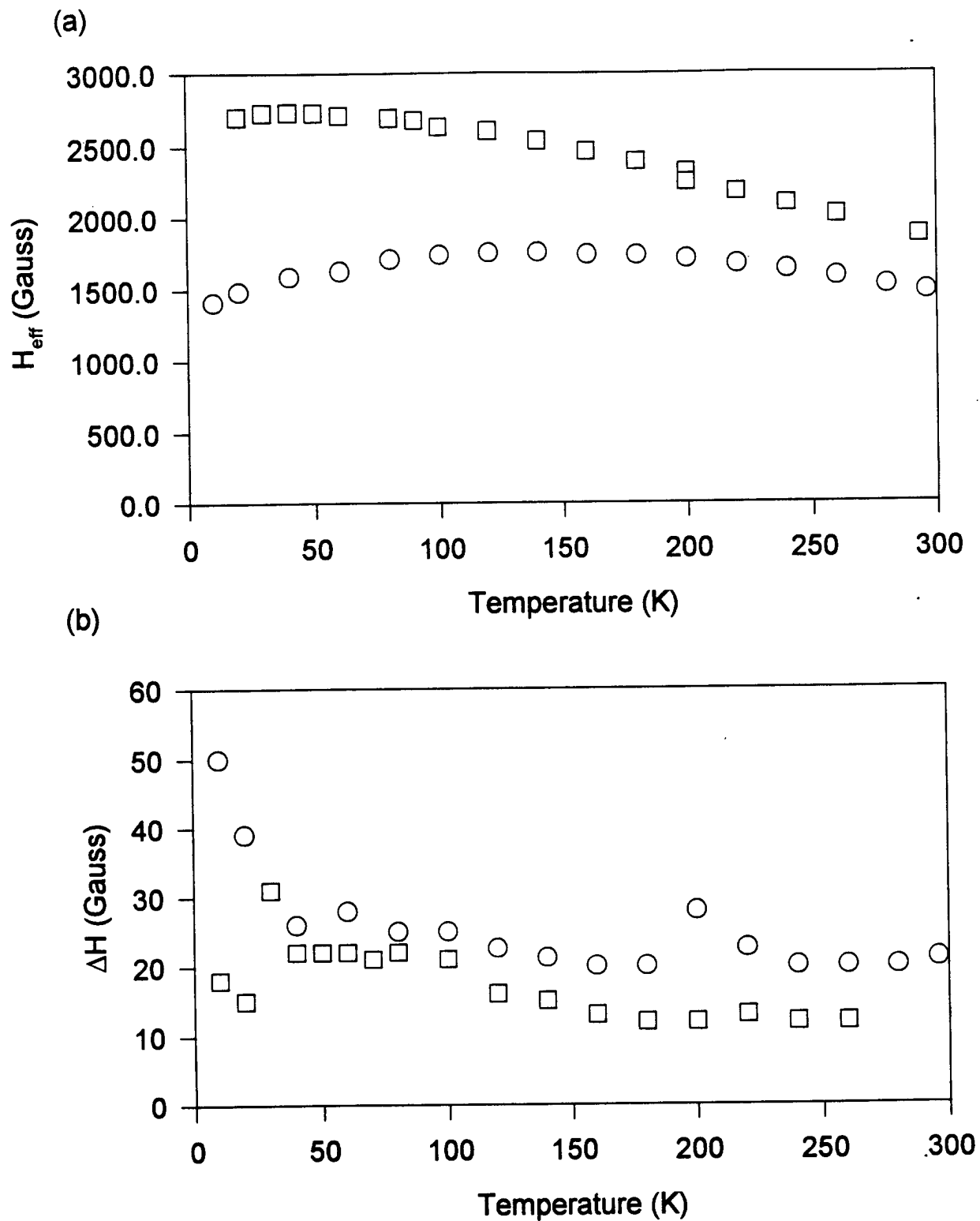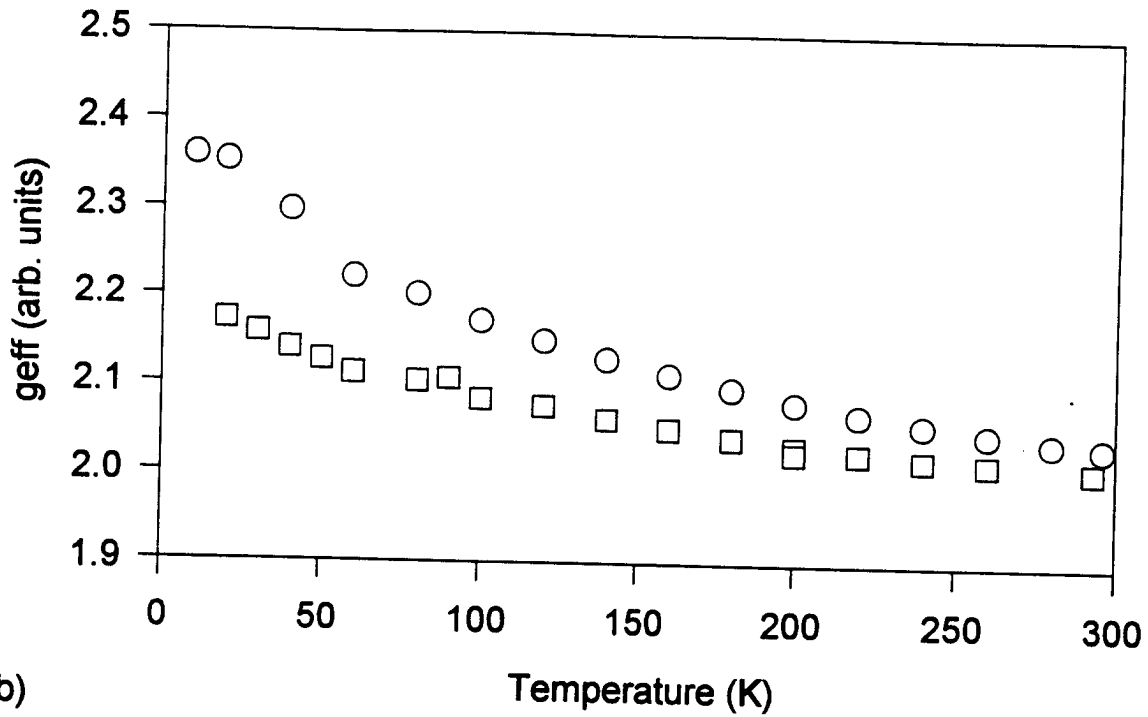
Figure 11. (a) The effective anisotropy field and (b) the in-plane FMR linewidth of $Ca_{0.24}$:YIG for both an as-grown sample - ○ and a sample annealed in N_2 at 1000 C for 7 hours - □
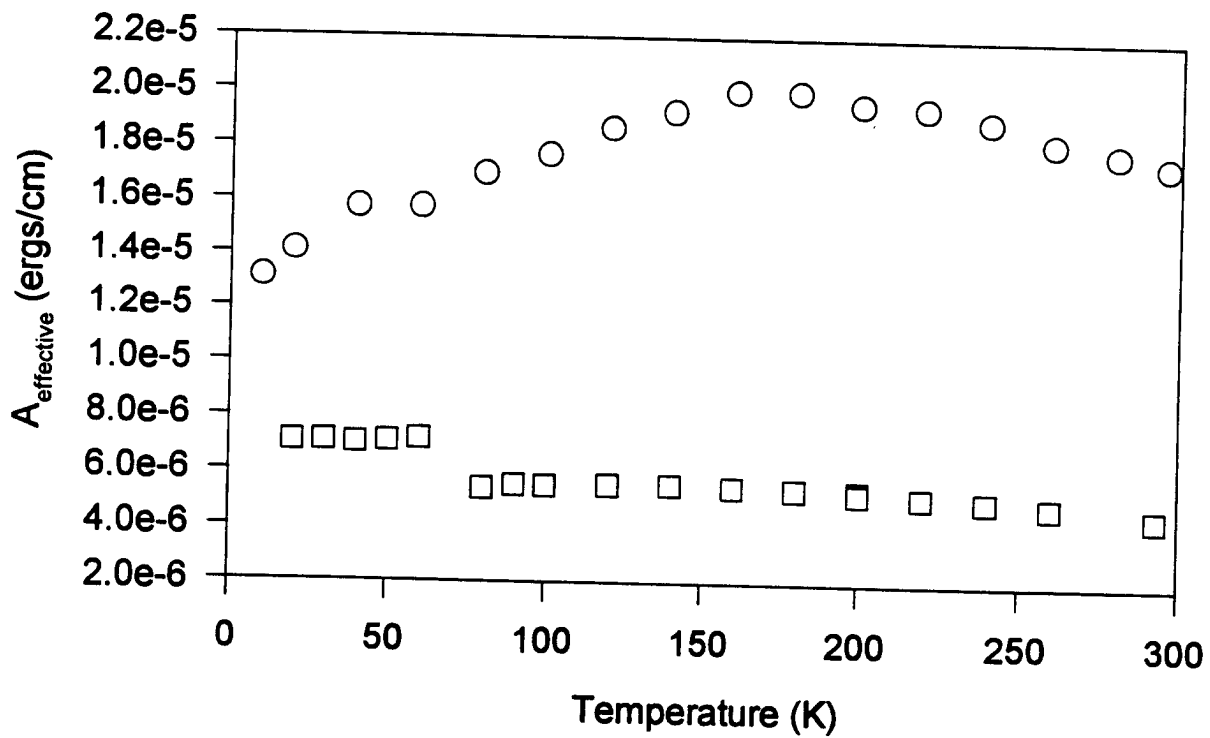
19

Figure 12. (a) The effective g-value and (b) the effective exchange constant of $Ca_{0.24}$:YIG for both an as-grown sample - O and a sample annealed in N_2 at 1000 C for 7 hours - □

in Figure 13 and indicates the position of the absorption edge. For $Ca_{0.34}$:YIG the band edge can be seen to occur at 2.5 eV while 2 peaks appear at 1.85 eV and 2.4 eV. In addition, a strong bleaching occurs above the absorption edge. It should be noted that Fe^{4+} has absorption peaks at 2.1 and 2.9 eV [11]. This would indicate that the Fe^{4+} must have an indirect effect. These peaks have been analyzed in a model assuming photon induced polaron hopping effect from one Fe^{3+} center to another. After the transition the excess energy is released to the lattice. At low temperatures, such an absorption process is expected to have a Gaussian lineshape peaked at a value of $4E_A$ where E_A represents the activation energy or the barrier height for the phonon-assisted hopping to occur [12, 13]. The lineshape will also have a half-width of $(8E_A\hbar\omega_0)^{1/2}$, where ω_0 is the frequency of the optical phonons involved in the polaron formation. A best fit of this model of the energy dependence for $Ca_{0.34}$:YIG at 10 K gives an activation energy of 0.46 eV and a phonon energy of 0.07 eV [14]. These are in agreement with activation energies of 0.2 to 0.4 eV found from DC conductivity measurements in the temperature range of 100 to 300 K and optical phonon modes which have been observed at 0.05 eV [10].

The absorption edge is also shifted by the dodecahedral substitution of Ca. In pure YIG, the absorption edge occurs at 2.8 eV, while in the $Ca_{0.34}$:YIG sample the absorption edge is reduced to 2.5 eV. It was verified that this was indeed the absorption edge by examining the energy dependence of the photoinduced conductivity as seen in Figure 14. The significant shift in the conductivity centered at 2.5 eV confirmed the position of the absorption edge.

G.   Magneto- optical Results

During the last year an experimental apparatus was completed, which is capable of measuring the Faraday rotation (FR) and magnetic circular dichroism (MCD) over the visible part of the light spectrum. Figures 15 displays the FR and MCD of a Ca:YIG film subjected to different high temperature annealing conditions. For increasing annealing temperature, the magnitude of the FR and MCD were suppressed increasingly at the shorter wavelengths. The peaks being suppressed in this regime appear to be the octahedral Fe^{3+} crystal field transitions, $^6A_{1g}(^6S) \rightarrow {}^4E_g;^4A_{1g}(G)$ at 467 nm, and $^6A_1(S) \rightarrow {}^4E;^4A_1(G)$ at 483 nm [15]. The non-uniformity of the suppression with wavelength indicates that the change is not simply due to the decrease in the magnetization that occurs with high temperature annealing, but rather a change in the oscillator strengths associated with the transitions.

H.   Reduction Study of Optical Absorption

Very recent optical absorption measurements over a sample successively annealed at various temperatures from 900 C to 1000 C have shown that the high temperature annealings produce broad changes in the optical absorption. This is shown in figure 16. The first low temperature annealings produce a decrease in the absorption, while it increases for successively higher annealing temperatures. Especially significant is the crossover for the 960 C annealing where the optical absorption goes from smaller than as-grown to larger that as-grown at around 850 nm. This would indicate that the annealings are affecting the high energy transitions due to crystal field transitions more so than the lower energy ones which is consistent with the above FR and MCD results.

As mentioned earlier in the report, "pickling" of the films results in a reversal in the
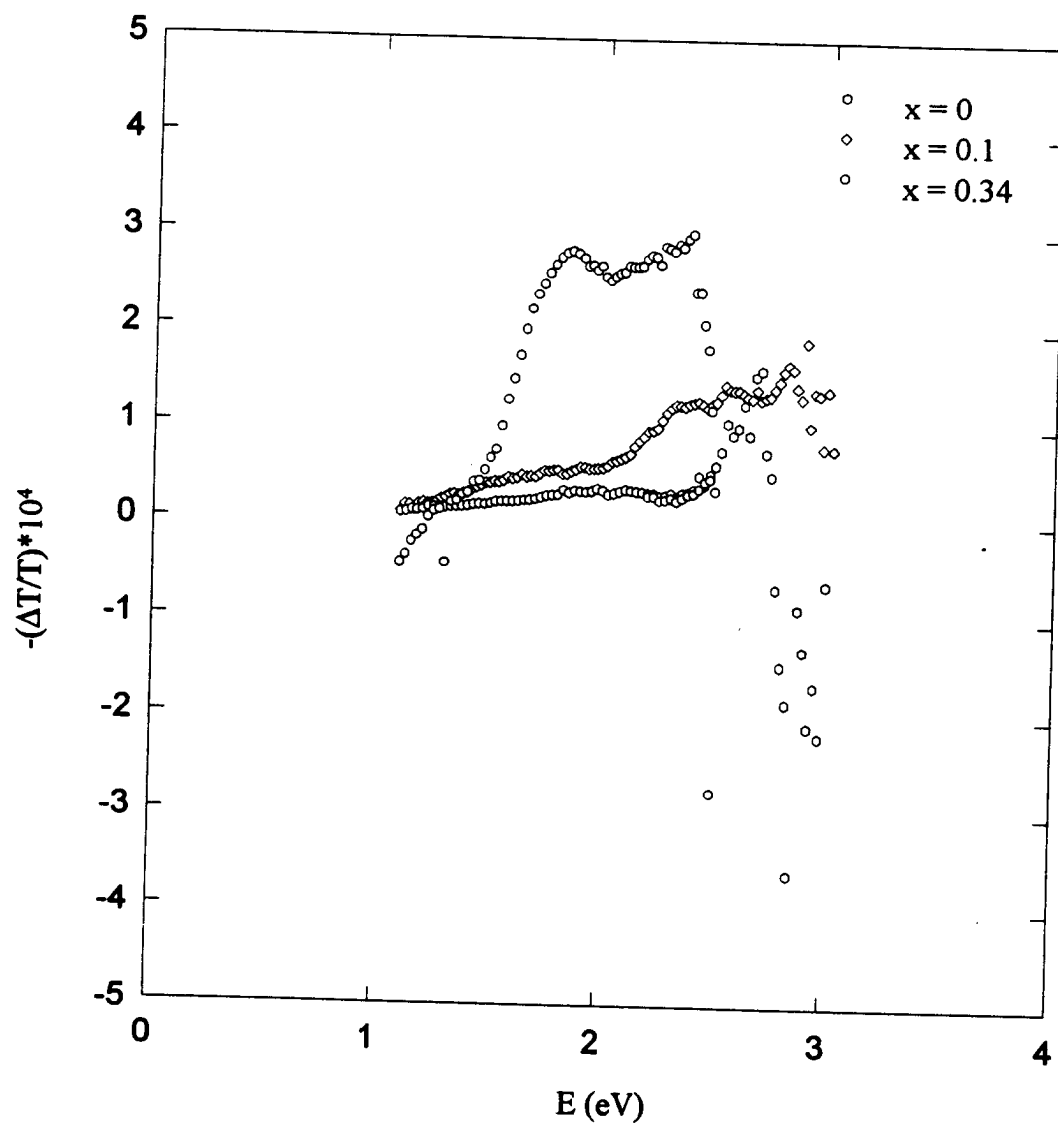
Figure 13. The photoinduced absorption spectra of
Ca_x:YIG at a pump energy of 3.4 eV taken at 10 K.
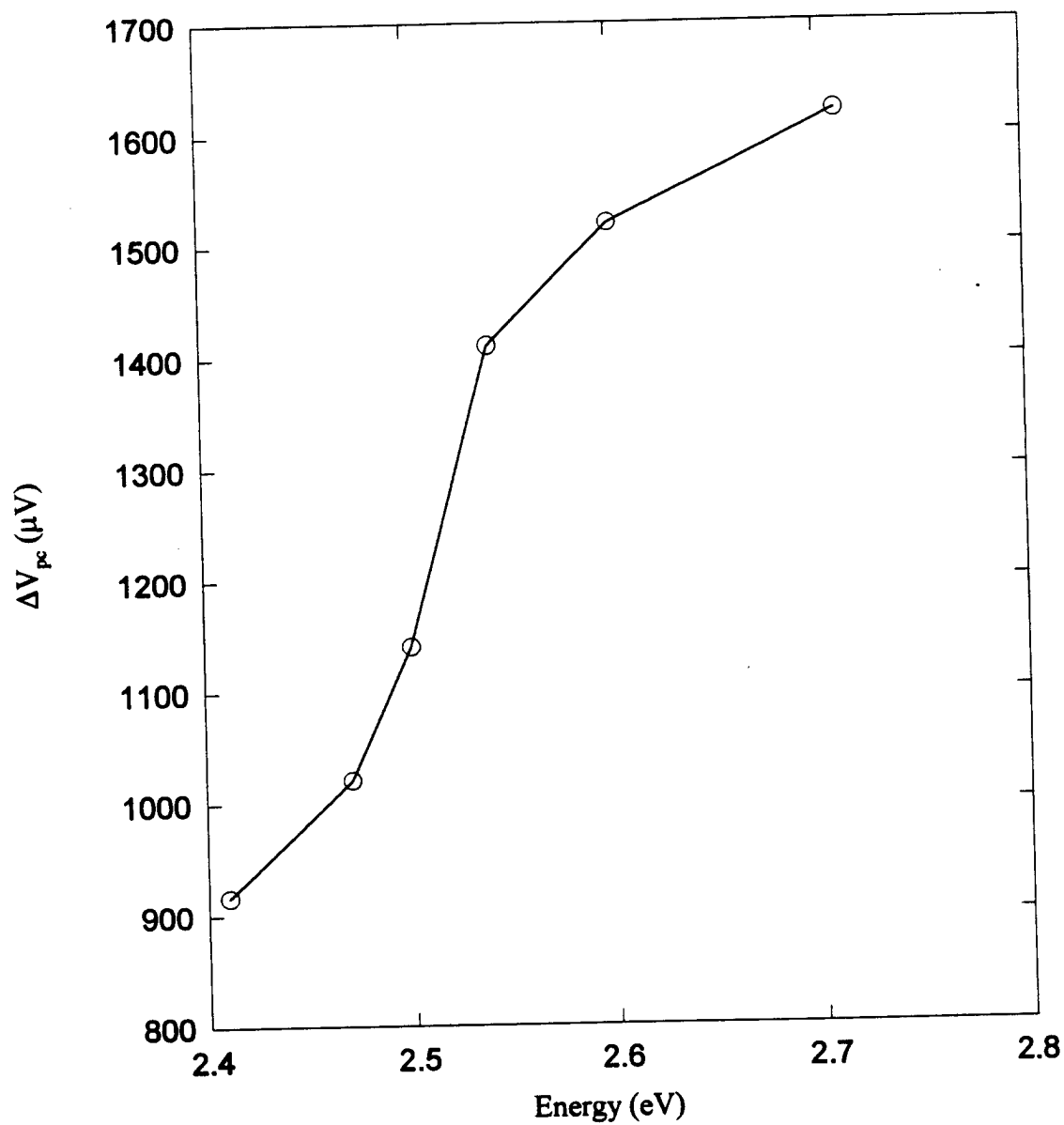
Figure 14. Photoconductivity of $Ca_{0.34}$:YIG

(a)

(b)

Figure 15. (a) The Faraday rotation and (b) the magnetic circular dichroism of $Ca_{0.24}$:YIG for both an as-grown sample - $\bigcirc$ and a sample annealed in N_2 at 1000 °C for 7 hours - $\square$

Figure 16. Optical absorption spectra of $Ca_{0.18}$:YIG for a sample successively annealed at the indicated temperatures in a N_2 atmosphere.

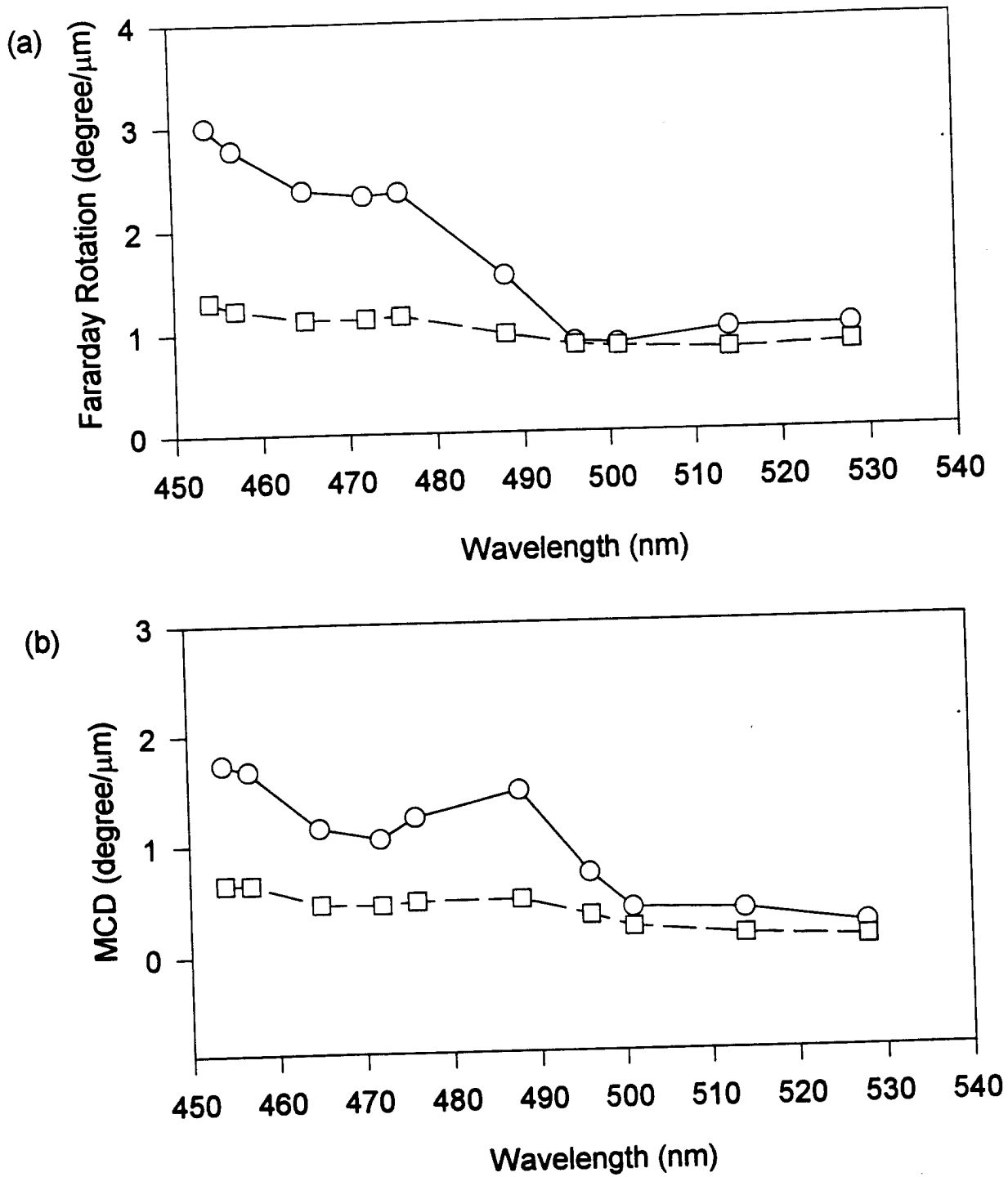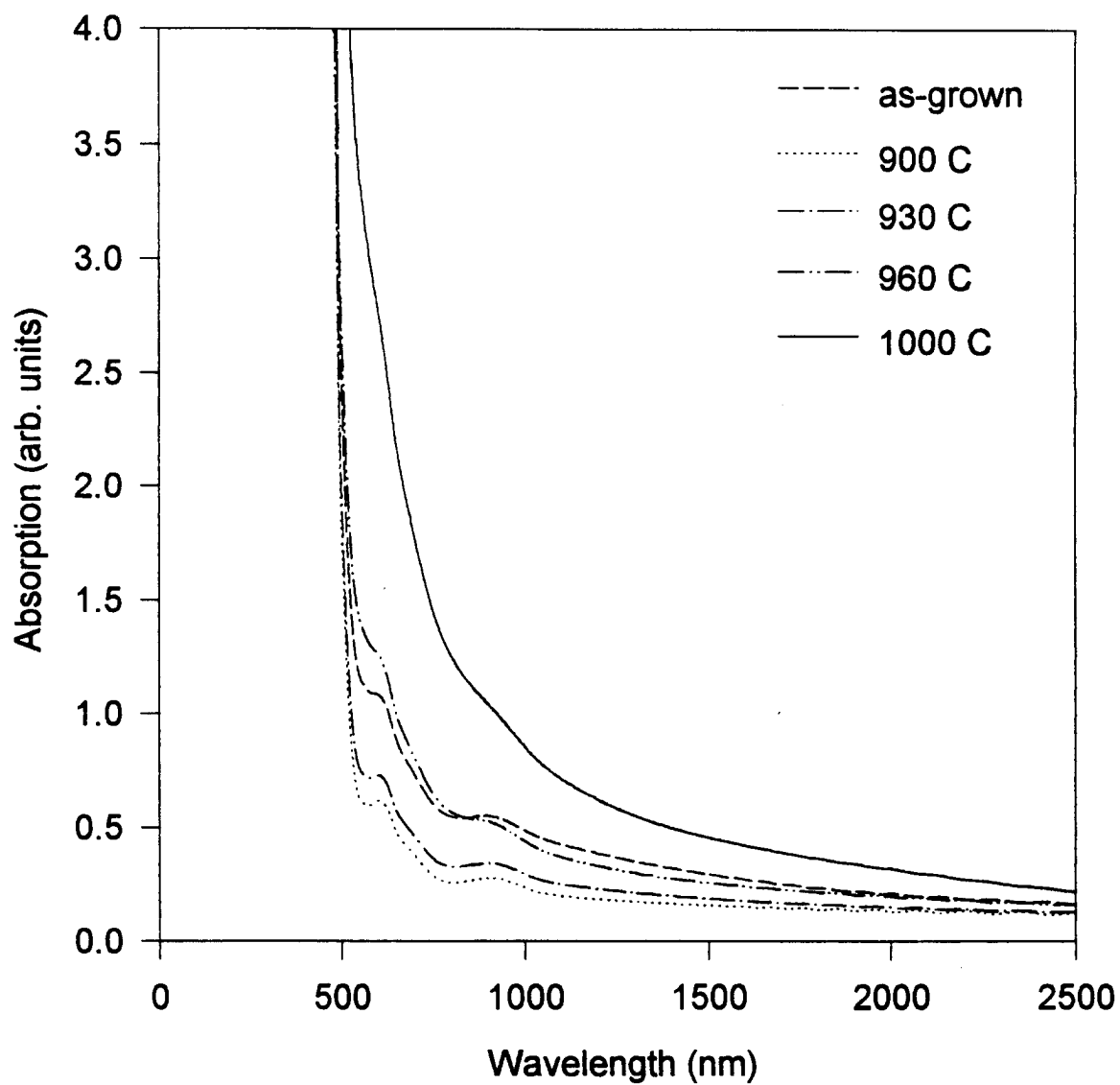change of the large increase in the resistivity. With this decrease in resistivity (and hence the modification of the Fermi energy), a reversal in the large increase in the optical absorption is expected. These complementary effects may allow the formation of regions of film in which different optical absorption occurs, with application as short wavelength rotators.

G.   Summary of Accomplishments

The LPE growth facility has been reestablished and 37 YIG based films of varying composition have been grown. A quantitative model of the surface layer resistivity in the doped YIG films has been proposed, from which the bulk resistivity of the film can be extracted from the I-V curves.

A comprehensive annealing study was carried out on $Ca_{0.2}$:YIG films which has enhanced the understanding of the role oxygen vacancies play in the magnetic, electric, and optical properties. This experiment has for the first time provided evidence that oxygen vacancies may mediate a ferromagnetic superexchange interaction and can be exclusively responsible for the low temperature anomaly. A quantitative molecular field model has been proposed and used to fit the magnetization vs. temperature curves to excellent agreement.

The large increases in both the resistivity and activation energy of the annealed films, as well as the spreading and increase of the optical absorption peak at 600 nm, indicate the existence of an oxygen impurity band centered at 0.3 eV above the valence band.

The annealed films have been induced into a RTHCS with conductivity increases up to seven orders of magnitude. A room temperature resistivity as low as 300 Ωcm has been achieved, with indication that a continuation of the process could reduce the resistivities by an additional order of magnitude. The presence of deep traps as the primary origin of the RTHCS was further evaluated by examining the RTHCS at multiple temperatures and fields. The results were consistent with this model.

A desire to explore the generality of the annealing effects led to an examination of a differently doped garnet films supplied by Airtron, Inc.. The annealing effects were shown to be consistent with those observed for the Ca:YIG study, and in addition a second order phase transition in the easy direction of magnetization was discovered for this material.

More recent measurements of the optical properties of the materials indicate, as with the magnetic and electric properties, broad changes in the optical absorption, FR and MCD. Evidence suggest that the reduction process affects the higher energy transitions more so than the transitions in the IR. Investigations of the optical properties of the "pickled" state are currently being performed. If, as expected, the optical properties of the "pickled" state revert to the as-grown values, application of structured electrode patterns should allow the films to be structured into optically distinct regions. The study of the traditional semiconducting properties of these films is continuing in conjunction with the newer optical investigation.

26

Appendix A : Recent Group Publications (since 1990)

1. "Photoinduced Absorption in Ca:YIG," A. Thavendrarajah, M. Pardavi-Horvath, and P.E. Wigen, *J. Apply. Phys.*, 67, 4941 (1990).

2. "Magnetic Superexchange in YIG and Ca^{2+}:YIG," A. Lehmann-Szweykowska, R. Wojceichowski, L. Pust, P.E. Wigen, and S. Batra, *Phys. Rev.*, **B43**, 3500 (1991).

3. "Polaronic Absorption in Uncompensated Cax:YIG," A. Thavendrarajah, Y. Song, and P.E. Wigen, *J. Appl. Phys.*, **70**, 6389 (1991).

4. "Spin Reorientation in $Tm_{2.14}Bi_{0.80}Pb_{0.06}Fe_{3.1}Ga_{1.9}O_{12}$ Thin Films," R.E. Bornfreund, D.C. Khan, P.E. Wigen, M. Pardavi-Horvath, J. Ings, and R. Belt, *IEEE Trans. Magn.*, **28**, 2991 (1992).

5. "Ferrimagnetism of Diamagnetically Substituted and Charge Compensated Ca^{2+} Substituted Yttrium Iron Garnet," M. Pardavi-Horvath, A. Thavendrarajah, P.E. Wigen, and P. DeGasperis, *J. Magn. and Magn. Mat.*, **119**, 193 (1993).

6. "Induced High Conduction State and Photomemory Effects in Partially Compensated Yttrium Iron Garnet," M. Pardavi-Horvath, S.H. Yuan, P.E. Wigen, and P. DeGasperis, *J. Magn. and Magn. Mat.*, **119**, 205 (1993).

7. "Effects of oxygen vacancies on the magnetic and the electrical properties of Ca-substituted yttrium iron garnet, " Y.J. Song, G.B. Turpin, R.E. Bornfreund, H. Aoyama, and P.E. Wigen, submitted for publication to the Journal of Magnetism and Magnetic Materials.

8. "Effects of a magnetic field on spin reorientation in BiGa:TmIG film, " R.E. Bornfreund, D.C. Khan, P.E. Wigen, M. Pardavi-Horvath, J.B. Ings, and R.F. Belt, to be published in Journal of Magnetism and Magnetic Materials.

9. "Room temperature high conduction state in annealed Ca-substituted yttrium iron garnet films,"G. B. Turpin, Y.J. Song, and P.E. Wigen, to be published in the International Conference on Magnetism proceedings in the Journal of Magnetism and Magnetic Materials.

Appendix B : Personnel Associated with ARO grant.
Former Personnel

      Dr. Ming Ye, Postdoctoral Researcher, presently employed at Supply Tech Incorporated, Ann Arbor, Michigan.
      Dr. Yong Jin Song, presently Dean of the College of Natural Science, Ajou Institute of Technology, Seoul, Korea.
      Dr. Ambalavanar Thavendrarajah, Assistant Professor, Department of Medical Physics, The Ohio State University, Columbus, Ohio.

Present Personnel

      Richard E. Bornfreund, Graduate Student
      George B. Turpin, Graduate Student
      Donglei Li, Graduate Student

MAGNETIC AND OPTICAL PROPERTIES OF UNCOMPENSATED CALCIUM SUBSTITUTED YTTRIUM IRON GARNET FILMS

DISSERTATION

Presented in Partial Fulfillment of the Requirements for
the Degree Doctor of Philosophy in the Graduate
School of The Ohio State University

By

A. Thavendrarajah, B.Sc.(Hons.), M.S.

* * * * *

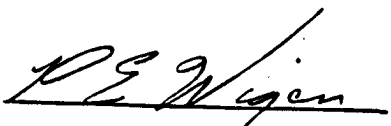The Ohio State University

1992

Reading Committee:

Professor P. E. Wigen

Professor R. Sooryakumar:

Professor B. R. Patton

Approved By

Dr. Philip E. Wigen, Advisor
Department of Physics

29

EFFECTS OF OXYGEN VACANCIES ON THE MAGNETIC AND THE ELECTRICAL PROPERTIES OF CA-SUBSTITUTED YTTRIUM IRON GARNET

DISSERTATION

Presented in Partial Fulfillment of the Requirements for the Degree
Doctor of Philosophy in the Graduate School of The Ohio State
University

By

Yong Jin Song, B.Sc, M.Sc

* * * * *

The Ohio State University

1993

Dissertation Committee

Philip E. Wigen

Robert L. Mills

Arthur J. Epstein

Adviser's Approval

_____

Adviser

Department of Physics

References

1. Y. J. Song, G. B. Turpin, R. E. Bornfreund, H. Aoyama and P. E. Wigen, JMMM (in press).
2. P. K. Larson and R. Metselaar, *Phys. Rev. B.*, **8**, 2016 (1973).
3. A. Lehmann-Szweykowska, R. Wojciechowski, L. Pust, P.E. Wigen, and S. Batra, *J. Appl. Phys.*, **69** (8), 4648 (1991).
4. Minoru M. Freund, Friedemann Freund and Francois Batllo, *Phys. Rev. Lett.*, **63**, 2096 (1987).
5. S.H. Yuan, M. Pardavi-Horvath, P.E. Wigen and P. DeGasperis, *J. Appl. Phys.*, **61**, 3552 (1987).
6. Private communication from Roger Belt, Airtron Inc.
7. R.E. Bornfreund, D.C. Khan, P.E. Wigen, M. Pardavi-Horvath, J. Ings, R. Belt, *IEEE Trans. Mag.*, **28**, 2991 (1992).
8. L.C. Hsai, thesis, The Ohio State University, 1981.
9. M. Marysko, P. Novak, J. Paces, and V. Volkov, *JMMM*, **104-107**, 429 (1992).
10. A. Thavendrarajah, Dissertation, (OSU 1992).
11. B.W. Faughnan, *Phys. Rev.*, **B4**, 3623 (1971).
12. W.B. Fowler, "Physics of Color Centers", Academic Press, NY, 1968.
13. T.H. Keil, *Phys. Rev.*, **140**, A601 (1965).
14. I.G. Austin and N.F. Mott, *Adv. Phys.*, **18**, 41 (1969).
15. J.P. Lascary, *Mat. Sci. Eng.*, **B16**, 228-234 (1993). E. Oh, A.K. Ramdas, and J.K. Furdyna, *J. Lum.*, **52**, 183-191, (1992).